J Polym Res (2011) 18:509–517
DOI 10.1007/s10965-010-9443-z

ORIGINAL PAPER

Modeling and optimization of a new impact-toughened epoxy nanocomposite using response surface methodology

Abdolreza Mirmohseni · Siamak Zavareh

Received: 6 January 2010 / Accepted: 21 April 2010 / Published online: 5 May 2010

Abstract This paper reports the development of a high-impact epoxy nanocomposite toughened by the combination of poly(acrylonitrile-*co*-butadiene-*co*-styrene) (ABS) as thermoplastic, clay as layered nanofiller, and nano-TiO_2 as particulate nanofiller. Response surface methodology (RSM) was applied for optimization and modeling of the impact strength of epoxy/ABS/clay/TiO_2 quaternary nanocomposite. A second-order mathematical model between the response (impact strength) and variables (ABS, clay and nano-TiO_2 contents) was derived. Analysis of variance (ANOVA) showed a high coefficient of determination value (R^2=98%). Under optimum conditions, maximum impact strength of 29.2 KJ/m^2 with 197% increase compared to neat epoxy was experimentally obtained. Also correlation between morphology and impact strength of the nanocomposite was investigated using scanning electron microscopy (SEM) and X-ray diffraction (XRD). A dispersion of exfoliated clay platelets, TiO_2 nanoparticles with low agglomeration and ABS nanoparticles was obtained as morphology of the nanocomposite. A new and more effective method for impact toughening of epoxy was introduced. This study clearly showed that the addition of the combination of layered and particulate nanofillers along with ABS as thermoplastic has a considerable enhancement effect on impact strength of epoxy.

Keywords Epoxy · Impact strength · RSM · Nanocomposite

A. Mirmohseni (✉) · S. Zavareh
Polymer Research Technology Laboratory, Department of Applied Chemistry, Faculty of Chemistry, University of Tabriz, Tabriz, Iran
e-mail: mirmohseni@tabrizu.ac.ir

Introduction

Epoxy resins are considered as one of the most important classes of thermosetting polymers. They are used extensively in protective coatings and structural applications including fiber reinforced composites, electrical laminates, casting, encapsulation, tooling and adhesives, because of their outstanding mechanical, thermal and electrical properties [1]. However, in all these applications, epoxy resins are brittle and rigid in nature and have poor resistance to crack propagation and low impact strength, so their many end use applications are limited [2]. Therefore, many investigations have been performed with the aim of toughening of epoxy polymers.

A common method for toughening epoxy resins is based upon blending with engineering thermoplastic polymers such as polysulfone [3], polyetherimide [4], and polyethersulfone [5]. Toughening with engineering thermoplastics has received much attention because it generally does not lead to a dramatic decrease in other desired mechanical properties [6]. Upon curing, thermoplastic phase separates from resin due to decrease in epoxy/thermoplastic compatibility. Improvement in toughness for epoxy/engineering thermoplastic is obtained only at higher thermoplastic content, where continuous or co-continuous phase morphology is formed. However, epoxy resins modified with higher thermoplastic content show a steep increase in viscosity which causes some difficulties in the handling of the resin [4, 5, 7].

Poly(acrylonitrile-*co*-butadiene-*co*-styrene) (ABS), a commercial thermoplastic with various applications, has been also used for epoxy toughening. Several studies have been performed on morphological and mechanical properties of epoxy/ABS hybrid. Two phase morphology, a dispersion of micron and sub-micron size ABS particles in

epoxy matrix, and sandwich morphology, a layer of thermoplastic wrapped in a skin of continuous epoxy material, have been obtained for cycloaliphatic amine cured epoxy/ABS blend [8–10]. In contrast with engineering thermoplastic toughened epoxies, it has been reported that the mechanical properties of epoxy/ABS hybrid improve at low ABS contents and decrease at higher loadings [11, 12].

An alternative approach for toughening is to fill epoxy cured polymers with inorganic nano-fillers to achieve nanocomposites. Nano-clay, a layered silicate, is widely used for enhancement of epoxy properties [13–17]. In addition to layered nano-fillers, various particulate ones such as silica (SiO_2) [18, 19], alumina (Al_2O_3) [20], titania (TiO_2) [21] and calcium carbonate ($CaCO_3$) [22] are also employed for this purpose. Incorporation of inorganic nano-fillers improves the fracture toughness to some extent. Increased toughness can be achieved up to certain fillers contents and further addition of them may not enhance toughness. Therefore, there is a limiting threshold for epoxy toughness using inorganic nano-fillers.

Recently, the thermoplastic polymers and clay modifiers have been employed together for epoxy toughening. In this respect, ternary nanocomposite based on hydroxyl terminated poly(ether ether ketone) with pendant methyl groups has been studied. Fracture toughness, tensile strength and modulus have been improved with the addition of the clay and reactive functionalized engineering polymer to epoxy resin, but impact strength has been decreased considerably [23]. Another report concerning enhancement of epoxy properties using a combination of polyamide and clay modifiers has been recently published. The hybrid composition containing 2% montmorillonite and 20% polyamide has exhibited maximum enhancement. Fracture toughness and impact strength of this ternary nanocomposite have been increased by 80% and 115%, respectively [24].

Epoxy/ABS/clay ternary nanocomposite has been studied in our previous work [25]. Addition of the combination of ABS and clay to epoxy has improved impact and tensile strengths considerably. In the present study, the combination of layered (clay) and particulate (TiO_2) nano-fillers along with thermoplastic (ABS) was added to epoxy matrix to study the effect of layered and particulate nano-fillers assembly in the presence of the thermoplastic on impact strength. It is also aimed to reduce the overall cost of the material preparation by using of inexpensive inorganic fillers. Response surface methodology (RSM) was applied to model the relationship between input variables (ABS, clay and nano-TiO_2 contents) and output response (impact strength), and to optimize the modifiers contents for preparation of the quaternary nanocomposite with maximum impact strength. To the best of our knowledge the present study is the first report on the addition of a combination of layered and particulate inorganic nanofiller, and thermoplastic to epoxy matrix for preparation of the quaternary nanocomposite. Morphological properties of the hybrid were investigated using X-ray diffraction (XRD) and scanning electron microscopy (SEM).

Experimental

Materials

Liquid Diglycidyl Ether of Bisphenol A (DGEBA) type epoxy resin, Epiran 6, with an epoxy equivalent weight of 187 eq/g, was purchased from Khuzestan Petrochemical Co. (Iran). The curing agent used was triethylene tetramine (TETA), supplied by Huntsman Chemical Products. Organically treated montmorillonite, Cloisite 30B, supplied by Southern Clay Products (USA), with methyl, tallow, bis(2-hydroxyethyl) quaternary ammonium ion as the cation exchange was used as nanofiller. Titanium dioxide (TiO_2) with an average diameter of 80 nm obtained from a local supplier was applied as particulate nano-filler for epoxy enhancement. A commercially available, general purpose grade ABS was obtained from Tabriz Petrochemical Co. (Iran). Mechanical properties of ABS are given in Table 1.

Preparation of specimens

In order to prepare epoxy thermosetting polymer, DGEBA type epoxy resin was mixed with 19% of curing agent for 10 min and degassed by a vacuum pump to remove the air bubbles. Optimum amount of hardener was selected according to maximum tensile and impact strengths of the prepared epoxy. The mixture was poured into silicon mould and cured for 24 h at room temperature followed by post-curing for 5 h at 75 °C and 2 h at 100 °C to ensure complete curing.

For preparation of epoxy/clay nanocomposite, the epoxy resin was mixed mechanically with the desired amount of the clay (Cloisite 30B) in a reaction kettle at 70 °C for 5 h. Then, it was sonicated for 10 min to disperse the clay in the resin. Relatively high operating temperature along with sonication facilitates the diffusion of oligomers inside the clay galleries. Proper time of the hot mixing and sonication for clay swelling was obtained using XRD studies. The

Table 1 Mechanical properties of general purpose ABS

Izod impact strength (KJ/m^2)	Tensile strength (MPa)	Vicat softening (°C)	MFI[a] (g/10min)	Rockwell hardness
35	45.0	102	1.5	105

[a] Melting flow index

mixture was degassed and cooled to room temperature. Then, a certain amount of the curing agent was added and mixed for 10 min. The mixture was degassed again, poured into a silicon mould and cured as the same method mentioned for epoxy thermosetting polymer prior to mechanical tests.

For blend preparation, a certain amount of ABS was dissolved in the epoxy oligomer at a temperature of 190 °C. Afterwards, the epoxy/ABS system was degassed and cooled to room temperature. Then hardener was added at desired ratio, mixed and degassed again. The curing procedure was the same. In order to prepare epoxy/ABS/clay and epoxy/ABS/TiO_2 ternary nanocomposites, ABS pellets were mechanically mixed with epoxy oligomer/clay or oligomer/TiO_2 system and dissolved at 190 °C and followed by curing procedure. For preparation of epoxy/ABS/clay/TiO_2 nanocomposite, a desired amount of ABS was mechanically mixed with epoxy/clay/TiO_2 system and dissolved at 190 °C. Then, the mixture was degassed and cured as before.

Characterization

The micrographs of the quaternary nanocomposite were taken on cut surfaces by using a Vega Tescan scanning electron microscope (Czech Republic). The sectioned surface of some samples was etched with dichloromethane for 10 h to observe phase morphology.

One-dimensional X-ray diffraction (XRD) patterns were obtained by using a Siemens D-500 X-ray diffractometer (Germany) with wavelength λ=1.54 Å (Cu-Kα), at a tube voltage of 35 KV, and tube current of 30 mA. The scanning angle range was from 2θ=2° to 45°.

The Izod impact strength was measured at room temperature for un-notched specimens with the dimensions of 63.5×12.7×7.2 mm as indicated in ASTM D256 using a Ceast-Resil impact tester (Italy). At least five replicates for each sample were tested. A measured weight of the material was poured into a leveled silicon mould and degassed completely using a powerful vacuum pump to prepare the homogeneous specimens.

Design of experiment

Response surface methodology (RSM) is a collection of statistical and mathematical techniques useful for modeling and optimization of a process in which a response of interest is influenced by several variables. It relates a response to a number of independent variables that affect the process output. The traditional optimization method examines a single factor at a time while fixing all other variables at one level. It is extremely time-consuming, expensive, and complicated processes for multi-variable systems. The RSM provides sufficient information on the effects of variables and overall experimental error with a minimum number of experiments [26].

In the present study, the most commonly used RSM design called central composite design (CCD) was selected for modeling and optimization of impact strength of the quaternary nanocomposite. The CCD permits the response surface to be modeled by fitting a second-order polynomial with the number of experiments equal to $2f + 2^f + n_c$, where f and n_c are the number of design factors and center runs, respectively. The CCD consists of three distinct portions: (1) 2f fractional points where the factor levels are coded to the usual low and high values (−1, +1); (2) axial points or "star" points on the axis of each variable at a distance α from the designed center where $\alpha = \left(2^f\right)^{1/4}$; and (3) center point that can be replicated to provide an estimate of experimental error variance. Therefore, each independent variable is varied at five levels (denoted as coded values $-\alpha$, −1, 0, +1, $+\alpha$.) [27].

Table 2 shows the coded and actual levels of the variables used to design the quaternary nanocomposite for this study. The input variables investigated were ABS content, clay content and nano-TiO_2 content. A total of 20 samples with different compositions were prepared in random order according to the CCD configuration for three-factor system with 6 replicates at the center point (Table 3).

The data obtained were then fitted to the following second-order polynomial equation:

$$Y = b_0 + \sum_{i=1}^{f} b_i x_i + \sum_{i=1}^{f} b_{ii} x_i^2 + \sum_{i=1}^{f-1} \sum_{j=i+1}^{f} b_{ij} x_i x_j \qquad (1)$$

where Y is the response or dependent variable (impact strength of the quaternary nanocomposite), b_0 is the offset term (constant), b_is are the linear coefficients, b_{ii}s are the quadratic coefficients, b_{ij}s are the interaction coefficients, x_i and x_j are the independent variables (the modifiers contents). The significance of the second-order model was evaluated by analysis of variance (ANOVA). The model was then used to optimize impact strength of the quaternary nanocomposite. Additional experiments were also carried

Table 2 Actual and coded levels of the design parameters

A. ABS content (%)	B. Clay content (%)	C. TiO_2 content (%)	Level code
2	2	2	−1.68
3	3	3	−1
4.5	4.5	4.5	0
6	6	6	+1
7	7	7	+1.68

Table 3 Experimental design and the corresponding response

Run No.	Experimental variables			Response
	ABS content (%)	Clay content (%)	TiO_2 content (%)	Impact strength (KJ/m^2)
1	3	3	3	24.0±3.5
2	6	6	6	20.3±3.1
3	3	3	3	15.1±1.8
4	6	6	6	12.3±2.0
5	3	3	3	15.5±1.9
6	6	6	6	13.3±1.7
7	3	3	3	14.1±1.5
8	6	6	6	12.2±1.0
9	2	4.5	4.5	15.3±1.6
10	7	4.5	4.5	9.7±0.8
11	4.5	2	4.5	22.0±3.3
12	4.5	7	4.5	14.4±2.3
13	4.5	4.5	2	20.7±3.6
14	4.5	4.5	7	14.5±1.6
15	4.5	4.5	4.5	17.5±1.9
16	4.5	4.5	4.5	17.4±2.3
17	4.5	4.5	4.5	17.3±2.5
18	4.5	4.5	4.5	18.2±2.2
19	4.5	4.5	4.5	17.5±2.1
20	4.5	4.5	4.5	16.3±1.5

out to verify predicted optimize conditions. Minitab software version 15 was used for analysis of variance (ANOVA) and regression coefficients calculations.

Results and discussion

Model fitting

The data in Table 3 were used to fit the mathematical model representing the impact strength (response) as a function of the modifiers contents (independent variables). The following equation expresses the overall predictive model in terms of the actual variables:

$$Y = 41.9478 + 5.1515A - 6.5033B - 5.7032C - 0.7810A^2 + 0.1147B^2 + 0.0204C^2 + 0.0667AB + 0.1333AC + 0.8000BC \quad (2)$$

where Y is the impact strength of the quaternary nanocomposite, and A, B and C are ABS, clay and nano-TiO_2 contents, respectively.

The adequacy of the regression model for explaining the experimental data at a 95% confidence level was explored from analysis of variance (ANOVA) results. The significance of main and interaction effects in the predictive model were considered based on their p-values (probability). The probability values less than 0.05 call for the rejection of the null hypothesis indicating that the particular term significantly affects the measured response of the system. The insignificant terms with p-values higher than 0.05 were removed from final expression of the model. Table 4 shows the probability values for overall and reduced model. The final predictive model (reduced model) in terms of the actual variables is shown in Eq. 3. The clay-TiO_2 interaction has significant effect on impact strength in the final model. Particulate nano-fillers can be self-assembled on the edge of clay layers and special layered-particulate nanostructure formed. It has been reported that such nanostructure exhibits a synergistic effect on reinforcing and toughening of epoxy thermosetting polymer [28].

$$Y = 35.1407 + 6.1613A - 5.1710B - 4.9193C - 0.7932A^2 + 0.8000BC \quad (3)$$

The ANOVA results (Table 5) indicated that the reduced model was highly significant, as p-value for the model was <0.0001. The coefficient of determination, R^2 for the reduced model was 98%. This indicated that only 2% of the total variability was not explained by the regressors in the model. The high R^2 value showed that the model obtained was able to give a good estimate of response of the system in the range studied. The insignificant "lack of fit" with p-value of 0.644 indicated that the model satisfactorily fitted the data. Furthermore, the plot of predicted values versus actual ones

Table 4 Effect examinations of the uncoded factors for overall and reduced model

Term	Overall model			Reduced model		
	SE[a]	t-value	*p*-value	SE[a]	t-value	*p*-value
Constant	3.63841	11.529	<0.0001	2.33650	15.040	<0.0001
A[b]	0.75577	6.816	<0.0001	0.60287	10.220	<0.0001
B[c]	0.75577	−8.605	<0.0001	0.41518	−12.455	<0.0001
C[d]	0.75577	−7.546	<0.0001	0.41518	−11.849	<0.0001
A×A	0.06045	−12.920	<0.0001	0.06601	−12.016	<0.0001
B×B	0.06045	1.898	0.087	–	–	–
C×C	0.06045	0.338	0.742	–	–	–
A×B	0.08113	0.822	0.430	–	–	–
A×C	0.08113	1.643	0.131	–	–	–
B×C	0.08113	9.861	<0.0001	0.08940	8.949	<0.0001

[a] Standard error
[b] ABS content
[c] Clay content
[d] Nano-TiO_2 content

(Fig. 1) showed satisfactory correlation between impact strength of the nanocomposite and modifiers contents.

Optimization of impact strength

As mentioned earlier, one of the aims of this study is to optimize the modifiers contents to obtain the quaternary nanocomposite with the highest impact strength. The optimum values of selected variables were obtained by solving the regression equation (Eq. 3). The optimum conditions for maximum impact strength were found to be as follow: ABS content of 3.9%, clay content of 2% and nano-TiO_2 content of 2%. The maximum impact strength predicted by using the optimum values of variables was 30.3 KJ/m^2. A verification of the predicted result was accomplished by performing the experiment using the set of optimized parameters. The experiment was repeated 5 times. The average impact strength obtained through the experiments was 29.2 KJ/m^2. Therefore, the experimental result was in close agreement with the model prediction. Increase in impact strength was higher than results of other published studies. Addition of both clay and poly(ether ether ketone) with pendant methyl groups to epoxy has decreased the impact strength significantly [23]. With 2% clay and 20% polyamide maximum improvement of 115% has been obtained [24]. In the present study, with much lower thermoplastic modifier (3.9% ABS), 2% clay and 2% nano-TiO_2 better results were observed.

Epoxy/ABS/clay ternary nanocomposite has been studied in our previous work [25]. Maximum impact strength of 22.8 KJ/m^2 with 133% increase compared to neat epoxy has been obtained for the ternary nanocomposite with optimum composition. The quaternary nanocomposite exhibited higher impact strength compared to the ternary nanocomposite. In the ternary system the clay (layered nano-filler) was added as inorganic nano-filler, whereas in the quaternary nanocomposite the combination of layered and particulate nano-filler (nano-TiO_2) was used. Therefore, the combination of clay and nano-TiO_2 had higher enhancement effect on impact strength than that of the clay alone. To our knowledge few papers concerning this topic have been presented. Addition of the combination of clay and nano-SiO_2 has exhibited synergistic effect on fracture toughness and tribological properties of epoxy resin but impact properties have not been studied yet [28]. In the present study, the effect of addition of the combination of layered and particulate nano-fillers along with ABS on impact strength was investigated.

Table 5 Analysis of variance results for the reduced model

Source	Degree of freedom	Sum of squares (SS)	Mean squares (MS)	*F*-value	*p*-value
Regression	5	231.320	46.2641	142.93	<0001
Linear	3	84.083	28.0278	86.59	<0001
Square	1	46.737	46.7370	144.39	<0001
Interaction	1	25.920	25.9200	80.08	<0001
Residual error	14	4.532	0.3237	–	–
Lack-of-fit	9	2.658	0.2954	0.79	0.644
Pure error	5	1.873	0.3747	–	–
Total	19	–	–	–	–

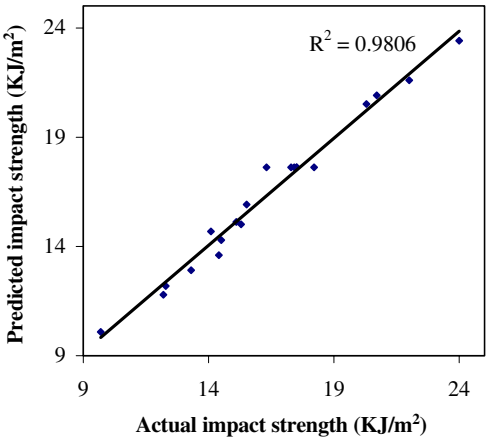

Fig. 1 Plot of predicted results of impact strength versus experimental values

Contour plots for impact strength of quaternary nanocomposite

Contour plots are usually used to observe the dependence of the response surface on the design factors. Contours are two-dimensional plots which are drawn as a function of two factors at a time, while holding all other factors at fixed levels (normally at the zero level). These plots that give a geometric representation of the underlying response function are helpful in understanding both the main and the interaction effects of factors.

Effect of ABS and clay loadings on impact strength

Figure 2 presents the surface response and contour plots for impact strength of the nanocomposite as a function of ABS content and clay loading while nano-TiO_2 content was maintained at 4.5%. According to the plots, ABS content and clay loading significantly affected impact strength of the nanocomposite. The impact strength increased with increasing ABS content to some extent and decreased with higher loadings, whereas the increase in clay loading decreased impact strength. The highest impact strength (22 KJ/m^2) was obtained for the nanocomposite with 2% clay loading and 4.5% ABS content.

The effect of ABS content on epoxy toughening has been studied. Impact strength of epoxy/ABS hybrid improves at low ABS contents and decreases at higher loadings [11, 12]. A dispersion of ABS particulates in epoxy matrix has been obtained as morphology of the hybrid. Nano-size ABS particles are formed in the hybrid with low ABS content. When ABS portion increases to higher loadings, ABS particles become larger and so particles are attached to each other and a continuous morphology formed. Nano-size ABS particles with larger aspect ratio and interface area between epoxy and ABS phases result in higher mechanical properties in comparison with continuous phase morphology [25].

As can be seen from Fig. 2, the impact strength decreases with increasing clay loading. Well-dispersed inorganic nano-fillers in low concentrations increase epoxy toughening. The presence of 4.5% nano-TiO_2 may cause agglomeration of the clay and TiO_2 nano-fillers and formation of the larger particles which can act as stress concentration sites for crack initiation and so decreases impact strength.

Effect of ABS and nano-TiO_2 loadings on impact strength

Figure 3 represents the 3D response surface and 2D contour plots for impact strength of the quaternary nanocomposite as a function of ABS and nano-TiO_2 contents. The clay loading was fixed at zero level (4.5%). It is obvious that the effect of ABS and nano-TiO_2 contents on the impact strength was similar to the effect of ABS and clay loadings.

Effect of clay and nano-TiO_2 loadings on impact strength

The effect of clay and nano-TiO_2 contents upon impact strength of the quaternary nanocomposite is depicted in Fig. 4. The ABS content was fixed at 4.5%. The response

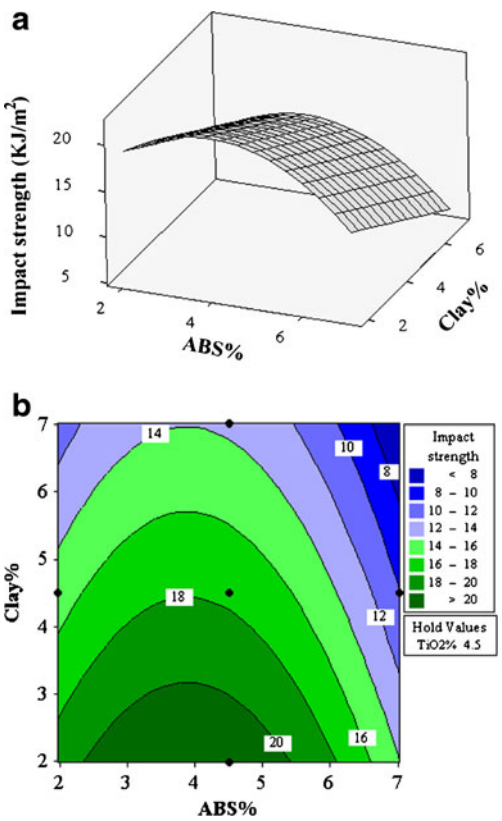

Fig. 2 **a** The response surface plot and **b** contour plot of the Impact strength as a function of ABS content and Clay content

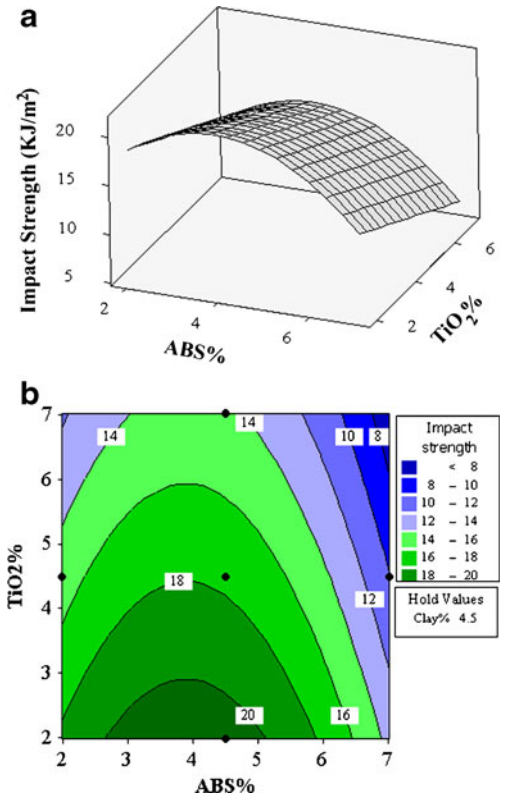

Fig. 3 **a** The response surface plot and **b** contour plot of the Impact strength as a function of ABS content and TiO_2 content

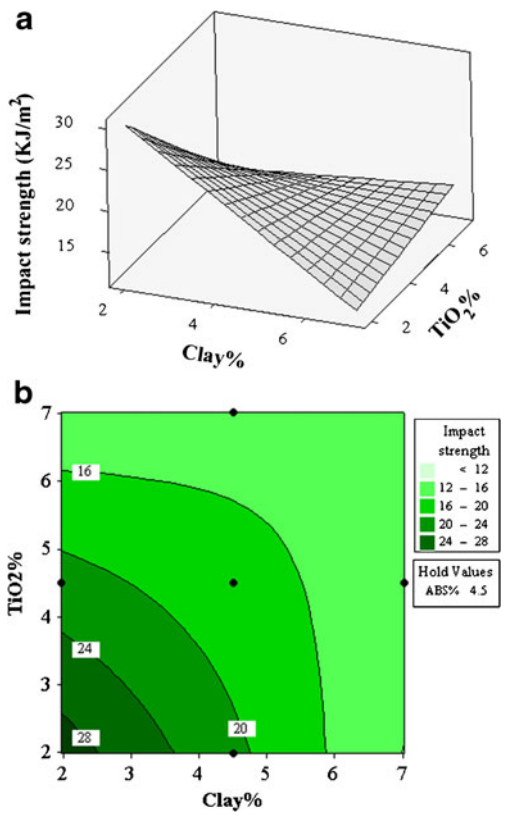

Fig. 4 **a** The response surface plot and **b** contour plot of the Impact strength as a function of TiO_2 content and Clay content

surface and contour plots in Fig. 4 show that a mutual interaction occurs between clay content and nano-TiO_2 content for impact strength of the nanocomposite as a response. It is clear from the figure that the impact strength decreases with the increase in clay and nano-TiO_2 contents.

Correlation between morphology and impact strength

Figure 5(a) presents X-ray diffraction patterns for pure clay (Cloisite 30B), epoxy/ABS hybrid and epoxy/ABS/clay/TiO_2 nanocomposite in the angle range of $2\theta=2–15°$. Epoxy/ABS system has no peak in its diffractogram due to its amorphous structure. The pure clay is characterized by (001) peak at $2\theta=4.81°$ corresponding to d-spacing of 1.83 nm. The absence of (001) peak in the X-ray spectrum of the nanocomposite indicates exfoliation of clay platelets in this material. The exfoliated clay structures result when the individual silicate layers are no longer close enough to interact with the adjacent layers' gallery cations. X-ray diffraction measurements can be used to characterize these

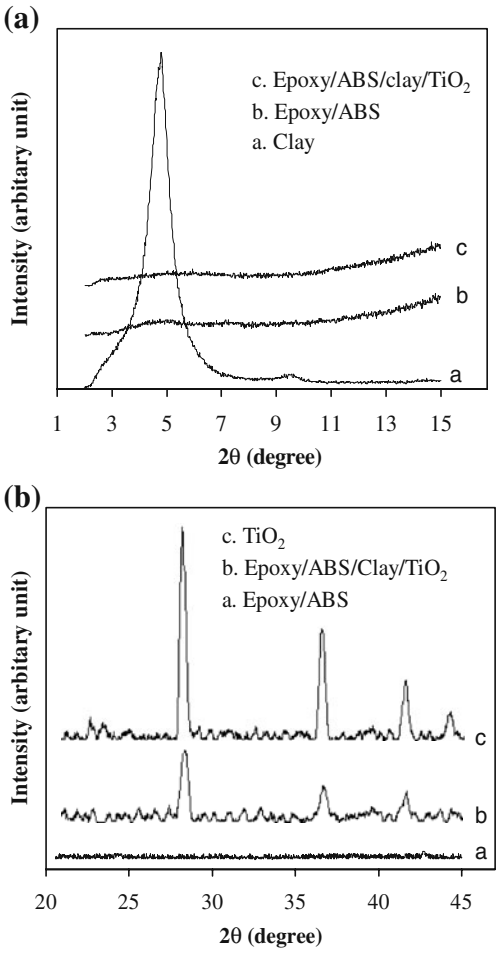

Fig. 5 XRD patterns for **a** clay, epoxy/ABS and epoxy/ABS/clay/TiO_2 in the angle range of 2–15°; and **b** TiO_2, epoxy/ABS/clay/TiO_2 in the angle range of 20–45°

nanostructures using clay (001) diffraction peaks. Such peaks indicate the d-spacing (basal spacing) of the clay layers in nanocomposite. If clay has exfoliated structure, no peaks are observed in the XRD due to the large d-spacing [29]. Figure 5(b) illustrates X-ray plots of the TiO_2 nanofiller, epoxy/ABS hybrid and quaternary nanocomposite in the angle range of $2\theta=20–45°$. For the TiO_2 sample, maximum reflection appears at $2\theta=27.5°$ which corresponds to the (110) peak of rutile crystalline phase based on standard values of pure rutile in the literature [30]. Epoxy/ABS has no peak in its spectrum because of its amorphous structure. The (110) characteristic of the TiO_2 also appears in the X-ray diffractogram of the quaternary nanocomposite which indicates the presence of the TiO_2 in the nanocomposite with no changes in its structure.

The micrograph of the cut surface of the quaternary nanocomposite with optimum composition is shown in the image (a) of Fig. 6. A dispersion of TiO_2 nanoparticles in epoxy/ABS/clay matrix with little agglomeration was observed. The micrograph of the etched sample is shown in the image (b) of Fig. 6. The cut surface was etched with dichloromethane to get a clear picture of the morphology for ABS phase in the nanocomposite. It was revealed that phase separation occurs and nano-size ABS particles are dispersed in epoxy rich matrix. High impact strength of prepared epoxy/ABS/clay/TiO_2 nanocomposite can be attributed to the dispersion of exfoliated clay nanoplatelets, TiO_2 nanoparticles and ABS nanoparticles which act as crack stoppers. ABS has been used as toughening modifier by other researchers and a dispersion of micron and sub-micron size ABS particles in the epoxy matrix has been obtained [8, 9]. Therefore, a new morphology was achieved for ABS phase in epoxy rich matrix. Nano-size ABS particulates with larger aspect ratio and interface area between epoxy and ABS phases resulted in higher mechanical properties in comparison with micron and sub-micron size ABS particles dispersion morphology. Unlike nano-size particles, micron-size particles can act as stress concentration sites for crack initiation and so provide lower toughening effect. Well-dispersed inorganic nanofillers such as exfoliated clay in low concentrations increase crack propagation and failure resistance through crack path deflection and micro-cracking mechanisms so improving epoxy toughening [13–15]. In the prepared nanocomposite, a dispersion of nano-size ABS and inorganic nano-fillers (clay and TiO_2) without agglomeration resulted in higher impact strength.

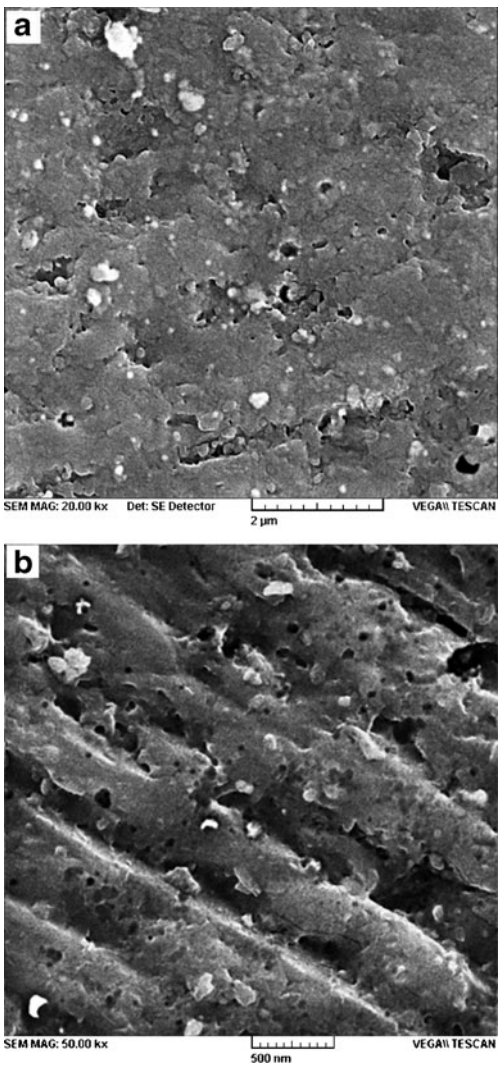

Fig. 6 SEM micrograph of epoxy/ABS/clay/TiO_2 quaternary nanocomposite **a** before and **b** after etching with dichloromethane

Conclusions

A new epoxy-based nanocomposite with higher impact strength was obtained. An empirical second-order model expressing the relationship between impact strength of the nanocomposite and modifiers contents was attained using response surface methodology. Analysis of variance showed a high coefficient of determination ($R^2=98\%$) and consequently a satisfactory adjustment of the regression model with the experimental data. The model was used to optimize modifiers contents to achieve maximum impact strength. The optimum values of the modifiers were found to be 3.9% ABS, 2% clay and 2% nano-TiO_2. The effect of modifiers on impact strength of the nanocomposite was established by the response surface and contour plots of the model-predicted responses. A dispersion of exfoliated clay nanoplatelets, TiO_2 and ABS nanoparticles in epoxy matrix were obtained as the morphology of the quaternary nanocomposite using XRD and SEM techniques.

Acknowledgement The authors are most grateful for the continuing financial support of this research project by University of Tabriz.

References

1. Muskopf JW, Mccollister SB (2002) In: Bohnet M, Brinker J, Cornils B et al (eds) Ullmann's encyclopedia of industrial chemistry, 6th edn. New York, Wiley
2. Lee H, Neville K (1967) Handbook of epoxy resins. McGraw Hill, New York
3. Yun NG, Won YG, Kim SC (2004) Polym Bull 52:365
4. Kimoto M, Mizutani K (1997) J Mater Sci 32:2479
5. Mimura K, Ito H, Fujioka H (2000) Polymer 41:4451
6. Bonnaud L, Pascault JP, Sautereau H (2004) Eur Polym J 40:2637
7. Chen C, Chen Y, Shen K et al (2003) J Polym Res 10:39
8. Lopez J, Ramirez C, Abad MJ (2002) J Appl Polym Sci 85:1277
9. Müller Y, Häuβler L, Pionteck J (2007) Macromol Symp 254:267
10. Abad MJ, Barral L, Cano J et al (2001) Eur Polym J 37:1613
11. Ramakrishna HV, Priya SP, Rai SK (2007) J Appl Polym Sci 104:171
12. Torres A, Lopez-de-Ullibarri I, Abad MJ et al (2004) J Appl Polym Sci 92:461
13. Wang L, Wang K, Chen L et al (2006) Compos A 37:1890
14. Kinloch AJ, Taylor AC (2006) J Mater Sci 41:3271
15. Zunjarrao SC, Sriraman R, Singh RP (2006) J Mater Sci 41:2219
16. Miyagawa H, Foo KH, Daniel IM et al (2005) J Appl Polym Sci 96:281
17. Mohan TP, Kumar MR, Velmurugan R (2006) J Mater Sci 41:2929
18. Zheng Y, Zheng Y, Nig R (2003) Mater Lett 27:2940
19. Ma J, Mo MS, Du X-Sh et al (2008) Polymer 49:3510
20. Shi G, Zhang MQ, Rong MZh (2004) Wear 256:1072
21. Wetzel B, Rosso P, Haupert F et al (2006) Eng Fract Mech 73:2375
22. Li L, Zou H, Shao L et al (2005) J Mater Sci 40:1297
23. Asif A, Leena K, Rao VL (2007) J Appl Polym Sci 106:2936
24. Bakar M, Wojtania I, Legocka I et al (2007) Adv Polym Technol 26:223
25. Mirmohseni A, Zavareh S (2010) J Polym Res 17:191
26. Khuri AI (2005) Response surface methodology and related topics. World Scientific Publishing Co. Pte. Ltd., Hockensack
27. Myers RH, Montgomery DC (2002) Response surface methodology: process and product optimization using designed experiments, 2nd edn. Wiley, USA
28. Jia Q, Zheng M, Cheng J et al (2006) Polym Int 55:1259
29. Gilman JW, Jackson CL, Morgan AB et al (2000) Chem Mater 12:1866
30. Brindley GW, Brown G (1980) Crystal structures of clay minerals and their X-ray identification. Mineralogical Society, London